Chinese Chemical Letters 37 (2026) 111924

Contents lists available at ScienceDirect

Chinese Chemical Letters

journal homepage: www.elsevier.com/locate/cclet

Thiophosphoryl pyridinol/pyrimidinol-based probes for covalent and fluorescent sensing of intracellular Cu^{2+}

Zhiyuan Qi[a,1], Jing Chen[a,1], Wenhao Xie[a,1], Zhibei Qu[a], Motonari Uesugi[a,b,*], Lu Zhou[a,c,*]

[a] School of Pharmacy, Fudan University, Shanghai 201203, China
[b] Institute for Chemical Research, Kyoto University, Uji, Kyoto 611-0011, Japan
[c] Quzhou Fudan Institute, Quzhou 324002, China

ARTICLE INFO

Article history:
Received 22 June 2025
Revised 28 September 2025
Accepted 29 September 2025
Available online 29 September 2025

Keywords:
Thiophosphorylated pyridinol/pyrimidinol
Activity-based sensing
Intracellular Cu^{2+}
Probes
Fluorescence imaging

ABSTRACT

Copper (Cu) is essential for life, with its redox cycling (Cu^{+}/Cu^{2+}) underpinning key biological processes. Although significant progress has been made in developing fluorescent probes for Cu^{+}, reliable tools for detecting intracellular Cu^{2+} remain limited, leaving a critical gap in the bioinorganic chemistry toolkit. To address this need, we developed an activity-based sensing (ABS) strategy for live-cell Cu^{2+} detection that leverages Cu^{2+}-dependent bioorthogonal conjugation. Specifically, we engineered thiophosphoryl pyridinol/pyrimidinol dyes that undergo Cu^{2+}-mediated activation, enabling covalent labeling of proximal proteins within intracellular Cu^{2+}-enriched microdomains and concomitant turn-on fluorescence. This work not only offers a powerful tool for detecting intracellular Cu^{2+} fluctuations under exogenous stimuli but also proposes thiophosphorylated pyridinol/pyrimidinol scaffolds as a versatile platform for future intracellular Cu^{2+} sensing applications.

© 2026 Published by Elsevier B.V. on behalf of Chinese Chemical Society and Institute of Materia Medica, Chinese Academy of Medical Sciences.

Copper ions are essential metal ions for life [1–3]. Through redox cycling between monovalent copper (Cu^{+}) and divalent copper (Cu^{2+}), they play catalytic roles in critical biological processes such as metabolism, proliferation, growth, and respiration [2,4–11]. Concurrently, clinical studies have demonstrated that dysregulation of copper-dependent redox activity is closely associated with pathological conditions including cancer [7], inflammatory immune responses [12,13], major neurodegenerative diseases [14], and hereditary disorders of copper metabolism [15,16]. Owing to the intracellular reducing environment, Cu^{+} predominates over Cu^{2+} within cells [17]. Consequently, fluorescence-based detection techniques targeting Cu^{+} have achieved significant advancements [18–27]. In contrast, Cu^{2+} exists at lower concentrations in living cells [17]. Additionally, Cu^{2+} exhibits paramagnetic properties, enabling strong fluorescence signal quenching through electron or energy transfer pathways [28,29]. Consequently, most Cu^{2+}-responsive probes operate *via* turn-off mechanisms [28,29]. That severely limited the visualization of Cu^{2+} and created substantial obstacles for investigating intracellular Cu^{2+} distribution, coordination interactions with proteins, and its correlations with various pathological factors.

Driven by the discovery of metal ion-mediated covalent modification of proteins by small molecules, chemists have developed activity-based sensing (ABS) strategies to address the pressing need for detecting intracellular metal ions and their responses to exogenous/endogenous stimuli [17,30,31]. These approaches leverage metal ion-triggered covalent reactions to achieve the spatial anchoring of probes through conjugation with proteins proximal to metal ion sites [17,30,31]. By leveraging Cu^{+}/Cu^{2+}-directed acyl imidazole strategies, scientists developed probes CD649 and CD649.2 for intracellular labile copper pools (Fig. 1) [17,30]. Upon Cu^{+}/Cu^{2+}coordination, the probes trigger Lewis acid activation of the acyl imidazole moiety, enabling covalent capture of proximal protein nucleophilic residues [30]. This mechanism allows for the spatial retention of the fluorophore while liberating fluorescence-quenching Cu^{2+} ions [17]. Therefore, this approach enables the real-time tracking of dynamic fluctuations in intracellular labile copper pools [17]. Notably, the CD649.2 exhibited dual selectivity for copper ions and the divalent oxidation state [17].

Although progress has been made in ABS-based copper ion probes, current strategies predominantly employ the acyl imidazole core framework, with a notable absence of alternative usable core structures. To address this limitation and explore alternative structural frameworks, we have developed a Cu^{2+}-

* Corresponding authors.
E-mail addresses: uesugi@scl.kyoto-u.ac.jp (M. Uesugi), zhoulu@fudan.edu.cn (L. Zhou).
[1] These authors contributed equally to this work.

https://doi.org/10.1016/j.cclet.2025.111924
1001-8417/© 2026 Published by Elsevier B.V. on behalf of Chinese Chemical Society and Institute of Materia Medica, Chinese Academy of Medical Sciences.

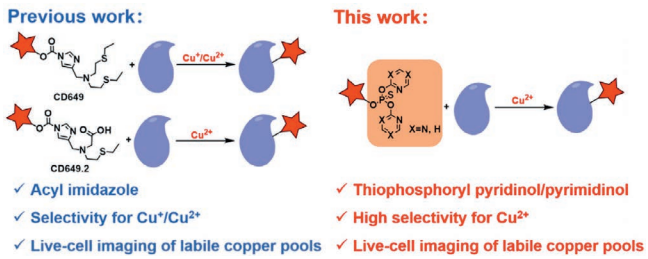


Fig. 1. Selective copper-responsive activity-based protein labeling.

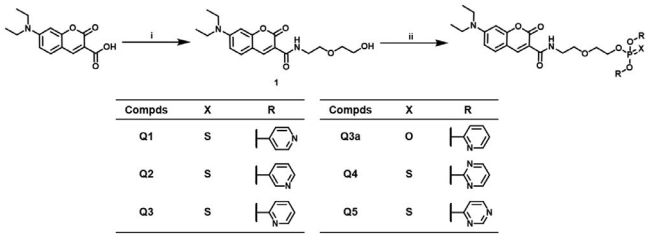


Fig. 2. Synthesis of **Q1**–**Q5**. Reagents and conditions: (i) 2-(2-aminoethoxy)ethanol, 2-(7-azabenzotriazol-1-yl)-*N*,*N*,*N*',*N*'-tetramethyluronium hexafluorophosphate (HATU), Et_3N, *N*,*N*-dimethylformamide (DMF), room temperature (RT). (ii) $PSCl_3$/$POCl_3$, R-OH, Et_3N, MeCN, 0 °C-RT.

directed covalent labeling strategy by using thiophosphoryl pyridinol/pyrimidinol as a reactive and dual Cu^{2+}-recognizing group. It reacts with nucleophilic lysine under alkaline conditions [32]. Both sulfur atom of thiophosphoryl and pyridine/pyrimidine rings are widely recognized as potent Cu^{2+} chelators and have been extensively utilized in probe design [33–35]. Coordination to the Lewis acidic Cu^{2+} center enhances the electrophilicity of the thiophosphoryl moiety, thereby inducing covalent conjugation with proteins (Fig. 1). This mechanism enables detection of Cu^{2+} fluctuations in labile copper pools within living cells under exogenous stimuli.

To develop Cu^{2+}-responsive ABS probes capable of proximal protein labeling, we designed target compounds **Q1**–**Q5** featuring a coumarin fluorophore, a diethylene glycol spacer, and thiophosphoryl pyridinol/pyrimidinol that integrate covalent anchoring and Cu^{2+}-coordination functionalities. The designed compounds were successfully synthesized *via* a two-step reaction routine (Fig. 2).

Next, we compared the activity of **Q1**–**Q5** under Cu^{2+}-catalyzed conditions. Sodium dodecyl sulfate polyacrylamide gel electrophoresis (SDS-PAGE) fluorescence imaging showed that compounds with *ortho*-positioned nitrogen (**Q3**, **Q4** and **Q5**) exhibited activity, whereas those lacking *ortho*-nitrogen (**Q1**, **Q2**) showed negligible activity (Fig. 3A). Furthermore, introduction of additional nitrogen atoms at either the *ortho* (**Q4**) or *para* position (**Q5**) enhanced activity compared to **Q3** (Fig. 3A). Comparative analysis of **Q3** and **Q3a** revealed that replacing the sulfur atom with an oxygen atom (**Q3a**) abolished the Cu^{2+}-catalyzed enhancement of labeling activity (Fig. 3B). These results demonstrated the critical importance of the *ortho*-positioned nitrogen atoms and sulfur atom.

To evaluate the Cu^{2+} selectivity of **Q3**–**Q5**, we performed fluorescent labeling assays using HeLa cell lysate as a proteomic substrate *in vitro*. The lysate was pre-incubated with various metal ions (250 μmol/L each) under physiological buffer conditions (50 mmol/L HEPES, pH 7.4) for 30 min. For the Fe^{2+} and Cu^{+} conditions, tris(2-carboxyethyl)phosphine (TCEP, 1000 μmol/L) was included as a reducing agent. Following the metal ion pretreatment, the samples were incubated with **Q3**–**Q5** (50 μmol/L) for 2 h at 20 °C. As shown in Fig. S1 (Supporting information), subsequent fluorescent scanning analysis of SDS-PAGE separated samples demonstrated that **Q3** (Fig. S1A), **Q4** (Fig. S1B), and **Q5** (Fig. 3C) exhibited Cu^{2+}-dependent covalent labeling of lysate proteins, with significantly higher efficiency than observed for other metal ions. Notably, even under conditions where Cu^{+} concentration is tenfold higher than that of Cu^{2+}, **Q5** remains inactive (Fig. S2 in Supporting information), demonstrating its high selectivity for Cu^{2+}.

Next, we examined the effects of various conditions on Cu^{2+}-dependent covalent labeling of proteins, including Cu^{2+} concentration and reaction time, as well as pH value and competition with copper chelators. As shown in Figs. S3 and S4 (Supporting information), the protein labeling of **Q5**, catalyzed by Cu^{2+} ions, exhibits dependence on Cu^{2+} concentration and reaction time, aligning well

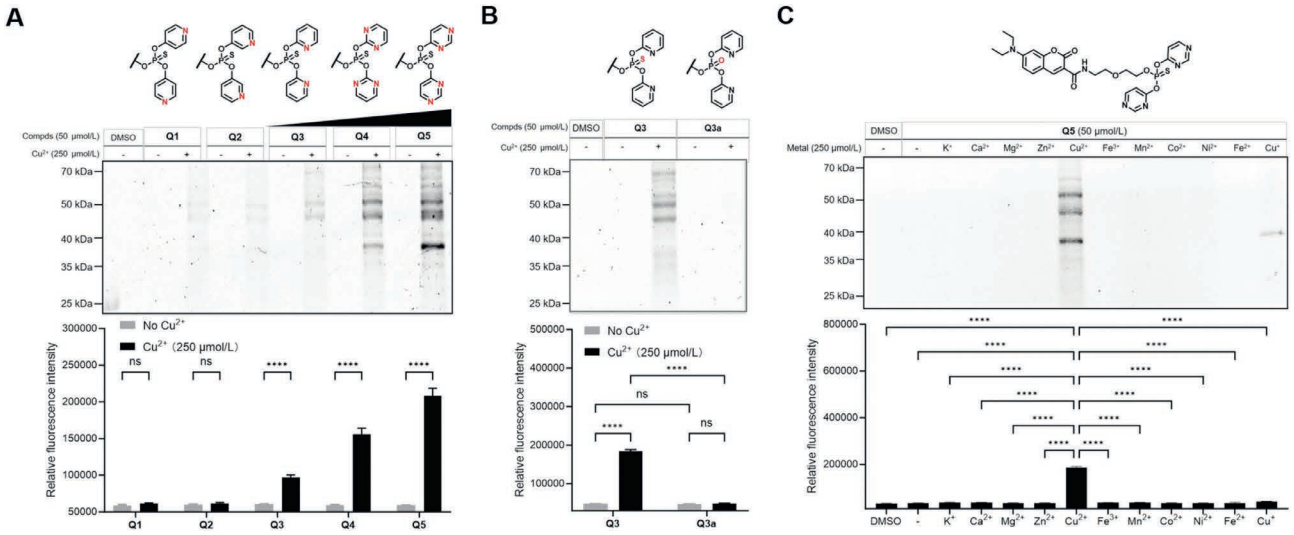


Fig. 3. (A) In-gel fluorescence image and relative fluorescence intensity of HeLa cell lysates treated by **Q1-Q5** (50 μmol/L) with or without $CuCl_2$ (250 μmol/L). (B) In-gel fluorescence image and relative fluorescence intensity of HeLa cell lysates treated by **Q3**/**Q3a** (50 μmol/L) with or without $CuCl_2$ (250 μmol/L). (C) In-gel fluorescence image and relative fluorescence intensity of HeLa cell lysates treated with **Q5** (50 μmol/L) and different metal ions (250 μmol/L). Cell lysate (0.5 g/L) was preincubated with 250 μmol/L metal ions for 30 min (Fe^{2+} and Cu^{+} groups supplemented with 1000 μmol/L TCEP as a reducing agent), followed by incubation with 50 μmol/L compounds at 20 °C for 2 h. In-gel fluorescence for SDS-PAGE was scanned by ChemiDoc MP and relative fluorescence intensity was analyzed in ImageJ. Error bars denote standard deviation (SD, $n = 5$). $^{****}P < 0.0001$. ns: no significance.

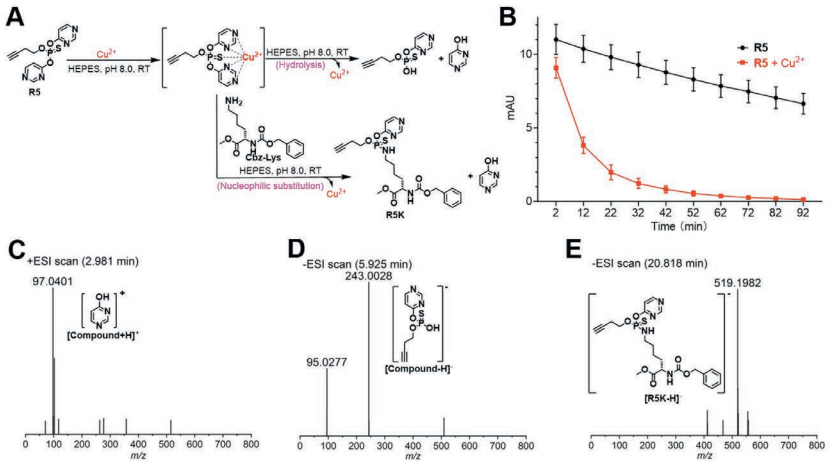


Fig. 4. (A) The binding of Cu^{2+} to thiophosphorylated pyrimidinol promotes **R5** hydrolysis or reacts with Cbz-Lys. (B) Effect of $CuCl_2$ (5 μmol/L) on the hydrolytic activity of **R5** (1 μmol/L) in HEPES buffer (pH 8.0). Error bars denote SD ($n = 5$). (C, D) High-resolution mass spectrometry (HRMS) spectra of **R5** (1 μmol/L) hydrolysis intermediates mediated by Cu^{2+} (5 μmol/L). (E) HRMS spectra of the product from the Cu^{2+}-catalyzed reaction between **R5** (5 μmol/L) and Cbz-Lys (0.5 μmol/L).

with the intended design (Figs. S3A and B). Further experimental results indicate that **Q5** labels proteins more readily under alkaline conditions (Fig. S3C). Additionally, Cu^{2+} chelator tris[(1-benzyl-1*H*-1,2,3-triazol-4-yl)methyl] amine (TBTA, Fig. S4B) inhibits the Cu^{2+}-dependent protein labeling of **Q5** in a concentration-dependent manner (Fig. S4A).

To delineate the underlying mechanism, we first evaluated the effect of Cu^{2+} on the hydrolytic activity of thiophosphoryl pyrimidinol. To circumvent potential interference from the coumarin moiety, we modified the **Q5** by replacing the coumarin group with a butynyl group, yielding the redesigned compound **R5** (Fig. 4A). Hydrolysis kinetics of **R5** (1 μmol/L) were subsequently analyzed in HEPES buffer (pH 8.0). High performance liquid chromatography (HPLC) monitoring revealed slow hydrolysis of **R5** under a mild alkaline condition, with ~30% degradation observed within 92 min (Fig. 4B). Notably, Cu^{2+} (5 μmol/L) dramatically accelerated this process, as evidenced by detectable hydrolysis within 2 min and complete degradation within 92 min (Fig. 4B). Liquid chromatography-mass spectrometry (LC-MS) analysis identified two hydrolysis products: pyrimidinol (*m/z* 97.0401 $[M+H]^+$, Fig. 4C) eluting at 2.9 min (Fig. S5 in Supporting information), and a thiophosphate intermediate (*m/z* 243.0028 $[M-H]^-$, Fig. 4D) eluting at 5.9 min (Fig. S5), corresponding to the hydrolysis of the thiophosphoryl pyrimidinol fragment. These results suggest that Cu^{2+} promotes the hydrolytic activation of the thiophosphoryl pyrimidinol unit, thereby potentiating the compounds' covalent protein-labeling activity.

Lysine is highly nucleophilic and predominantly located on protein surfaces, making it an accessible target for covalent reagents and probes [31,36,37]. To examine Cu^{2+}-dependent lysine modification by **R5**, we conducted LC-MS analyses of **R5** (5 μmol/L) and Cbz-Lys (0.5 μmol/L, Fig. 4A) reaction in the presence of Cu^{2+} (25 μmol/L) (Fig. S6A in Supporting information). The product detected (*m/z* 519.1982 $[M-H]^-$, Fig. 4E) was confirmed as **R5K** (a thiophosphorylated lysine adduct) by comparison with a synthetic standard (Fig. S7 in Supporting information). Critically, no **R5K** formation was observed under Cu^{2+}-free conditions, even after 12 h of incubation during which **R5** had fully been hydrolyzed (Fig. S6B in Supporting information). Collectively, these mechanistic studies demonstrate that Cu^{2+} binding enhances the reactivity of the thiophosphorylated pyrimidinol moiety, promoting either hydrolysis or lysine conjugation (Fig. 4A).

Building on the Cu^{2+} selectivity of the compounds, we further investigated their ability to detect changes in intracellular Cu^{2+} levels. Among the tested compounds, **Q5** exhibited the highest

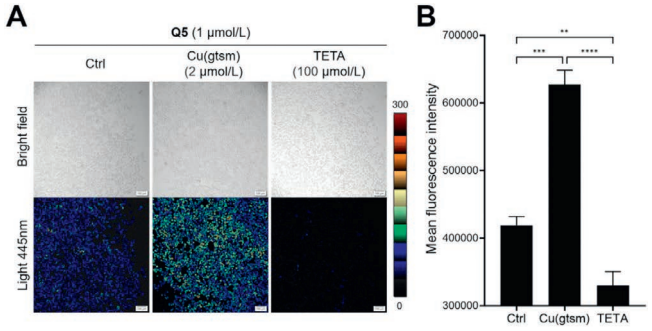


Fig. 5. Fluorescence imaging of labile Cu^{2+} pools in live HeLa cells using **Q5**. (A) HeLa cells treated with solvent vehicle control, the ionophore Cu(gtsm) (2 μmol/L) for 2 h or the chelator TETA (100 μmol/L) for 12 h. Cells were washed twice with PBS, incubated with **Q5** (1 μmol/L) for 1 h, washed twice with PBS, and then imaged. (B) Mean fluorescence intensity of the HeLa cells. Fluorescence intensity of **Q5** was determined from experiments performed in triplicate with $\lambda_{ex} = 445$ nm. Mean fluorescence intensity was analyzed in ImageJ. Error bars denote SD ($n = 5$). Scale bar: 100 μm. $^{**}P < 0.01$, $^{***}P < 0.001$, $^{****}P < 0.0001$.

Cu^{2+}-catalyzed activity *in vitro* (Fig. 3A). As shown in Figs. S8 and S9 (Supporting information), further cellular experiments and stability assays confirmed the low cytotoxicity of **Q5** toward HeLa cells (50% cytotoxic concentration (CC_{50}) = 75 ± 0.41 μmol/L, Fig. S8) and its slow hydrolysis under physiological conditions (phosphate buffered saline (PBS), pH 7.4, 37 °C, Fig. S9). These results prompting the selection of **Q5** for monitoring intracellular Cu^{2+} fluctuations. To validate its responsiveness, intracellular Cu^{2+} levels were modulated by pre-incubation with Cu(gtsm) (2 μmol/L) (a membrane-permeable Cu^{2+} ionophore, Fig. S10 in Supporting information) to elevate Cu^{2+} pools or treatment with TETA (100 μmol/L) (triethylenetetramine, a high-affinity Cu^{2+} chelator, Fig. S10) to deplete endogenous Cu^{2+}, followed by incubation with **Q5** (1 μmol/L). Live-cell fluorescence imaging revealed distinct Cu^{2+}-dependent responses. Cu(gtsm)-treated cells showed markedly enhanced fluorescence compared to untreated control (Figs. 5A and B). TETA-treated cells exhibited significant fluorescence attenuation (Figs. 5A and B). The trend that cellular fluorescence intensity changes of **Q5** is similar to that of the Cu^{2+} probe *N*-aminofluorescein (Fig. S11 in Supporting information) [38–40]. These results conclusively demonstrate that **Q5** serves as a reliable probe for monitoring the changes of labile Cu^{2+} levels in living cells. Subcellular co-localization experiments demonstrated that **Q5** localizes to endoplasmic reticulum, lysosomes, and mitochondria (Fig. S12 in Supporting information).

In summary, we have successfully developed a novel class of Cu^{2+}-dependent probes based on activity-driven labeling by thiophosphoryl pyridinol/pyrimidinol. Fluorescence labeling assays in cell lysates demonstrated the high selectivity of compounds for Cu^{2+}. Mechanistic studies revealed that Cu^{2+} enhances the hydrolytic activation of the thiophosphoryl pyrimidinol, which catalyzes compounds to react with lysine residues, thereby enhancing protein-targeted labeling efficacy. Intracellular fluorescence imaging experiments demonstrated that **Q5** enables the detection of Cu^{2+} fluctuations in living cells under exogenous stimuli. This study provided the thiophosphoryl pyridinol/pyrimidinol as a functional group for detecting labile Cu^{2+} levels in live cells, laying a solid foundation for the broader application of such chemotypes in chemical biology.

CRediT authorship contribution statement

Zhiyuan Qi: Writing – review & editing, Writing – original draft, Validation, Methodology, Investigation, Formal analysis, Data curation. **Jing Chen:** Methodology, Investigation, Formal analysis, Data curation. **Wenhao Xie:** Writing – review & editing, Data curation. **Zhibei Qu:** Supervision, Formal analysis. **Motonari Uesugi:** Writing – review & editing, Writing – original draft, Supervision, Project administration, Formal analysis. **Lu Zhou:** Writing – review & editing, Writing – original draft, Supervision, Resources, Project administration, Funding acquisition, Formal analysis, Conceptualization.

Declaration of competing interest

The authors declare that they have no known competing financial interests or personal relationships that could have appeared to influence the work reported in this paper.

Acknowledgments

This study was supported by the National Key R&D Program of China (No. 2023YFC3603303), the National Natural Science Foundation of China (No. U24A20524), and Shanghai Municipal Committee of Science and Technology (No. 21TQ016).

Supplementary materials

Supplementary material associated with this article can be found, in the online version, at doi:10.1016/j.cclet.2025.111924.

References

[1] S.M. Adam, G.B. Wijeratne, P.J. Rogler, et al., Chem. Rev. 118 (2018) 10840–11022.
[2] A.V. Davis, T.V. O'Halloran, Nat. Chem. Biol. 4 (2008) 148–151.
[3] E.L. Que, D.W. Domaille, C.J. Chang, Chem. Rev. 108 (2008) 1517–1549.
[4] C.M. Ackerman, C.J. Chang, J. Biol. Chem. 293 (2018) 4628–4635.
[5] C.J. Chang, Nat. Chem. Biol. 11 (2015) 744–747.
[6] L. Chen, J. Min, F. Wang, Signal Transduct. Target. Ther. 7 (2022) 378.
[7] E.J. Ge, A.I. Bush, A. Casini, et al., Nat. Rev. Cancer 22 (2022) 102–113.
[8] F.P. Guengerich, J. Biol. Chem. 293 (2018) 4603–4605.
[9] K.M. Lancaster, S. DeBeer George, K. Yokoyama, et al., Nat. Chem. 1 (2009) 711–715.
[10] M.L. Schlief, A.M. Craig, J.D. Gitlin, J. Neurosci. 25 (2005) 239–246.
[11] L. Zhao, J. Li, G. Chen, et al., Chin. Chem. Lett. 37 (2026) 110959.
[12] E.W. Hunsaker, K.J. Franz, Inorg. Chem. 58 (2019) 13528–13545.
[13] C. White, J. Lee, T. Kambe, et al., J. Biol. Chem. 284 (2009) 33949–33956.
[14] K.J. Barnham, A.I. Bush, Chem. Soc. Rev. 43 (2014) 6727–6749.
[15] S.G. Kaler, Nat. Rev. Neurol. 7 (2011) 15–29.
[16] S. Lutsenko, Biochem. Soc. Trans. 36 (2008) 1233–1238.
[17] A.T. Pezacki, C.D. Matier, X. Gu, et al., Proc. Natl. Acad. Sci. U. S. A. 119 (2022) e2202736119.
[18] C.M. Ackerman, S. Lee, C.J. Chang, Anal. Chem. 89 (2017) 22–41.
[19] S.C. Dodani, D.W. Domaille, C.I. Nam, et al., Proc. Natl. Acad. Sci. U. S. A. 108 (2011) 5980–5985.
[20] S.C. Dodani, A. Firl, J. Chan, et al., Proc. Natl. Acad. Sci. U. S. A. 111 (2014) 16280–16285.
[21] D.W. Domaille, E.L. Que, C.J. Chang, Nat. Chem. Biol. 4 (2008) 168–175.
[22] D.W. Domaille, L. Zeng, C.J. Chang, J. Am. Chem. Soc. 132 (2010) 1194–1195.
[23] T. Hirayama, G.C. Van de Bittner, L.W. Gray, et al., Proc. Natl. Acad. Sci. U. S. A. 109 (2012) 2228–2233.
[24] M. Taki, S. Iyoshi, A. Ojida, et al., J. Am. Chem. Soc. 132 (2010) 5938–5939.
[25] T. Xiao, C.M. Ackerman, E.C. Carroll, et al., Nat. Chem. Biol. 14 (2018) 655–663.
[26] L. Yang, R. McRae, M.M. Henary, et al., Proc. Natl. Acad. Sci. U. S. A. 102 (2005) 11179–11184.
[27] L. Zeng, E.W. Miller, A. Pralle, et al., J. Am. Chem. Soc. 128 (2006) 10–11.
[28] K.P. Carter, A.M. Young, A.E. Palmer, Chem. Rev. 114 (2014) 4564–4601.
[29] E. Falcone, A. Sour, V. Lebrun, et al., Dalton Trans. 48 (2019) 14233–14237.
[30] S. Lee, C.Y. Chung, P. Liu, et al., J. Am. Chem. Soc. 142 (2020) 14993–15003.
[31] T. Miki, M. Awa, Y. Nishikawa, et al., Nat. Methods 13 (2016) 931–937.
[32] F.H. Lu, P. Yue, X.R. Wang, Z.L. Lu, Inorg. Chem. Commun. 34 (2013) 19–22.
[33] M.L. Giuffrida, G. Trusso Sfrazzetto, C. Satriano, et al., Inorg. Chem. 57 (2018) 2365–2368.
[34] M. Kaur, Y.H. Ahn, K. Choi, et al., Org. Biomol. Chem. 13 (2015) 7149–7153.
[35] W.L. Lee, T.W. Hsu, W.C. Hung, J.M. Fang, Dalton Trans. 48 (2019) 8026–8029.
[36] S.R. Adusumalli, D.G. Rawale, K. Thakur, et al., Angew. Chem. Int. Ed. 59 (2020) 10332–10336.
[37] N.C. Reddy, M. Kumar, R. Molla, V. Rai, Org. Biomol. Chem. 18 (2020) 4669–4691.
[38] X. Chen, H. Ma, Anal. Chim. Acta 575 (2006) 217–222.
[39] J. Xu, Y. Hou, Q. Ma, et al., Spectrochim. Acta A: Mol. Biomol. Spectrosc. 124 (2014) 416–422.
[40] H.T. Zhi, Z. Lu, L. Chen, et al., Bioorg. Chem. 147 (2024) 107421.